

## Research Article

# Experimental Study on Mechanical Properties of Briquette Coal Samples with Different Moisture Content

Wang Haidong,<sup>1</sup> Tao Yang ,<sup>1</sup> Wang Deyue,<sup>2</sup> Sun Xin,<sup>1</sup> and Gao Jiahui<sup>1</sup>

<sup>1</sup>School of Safety, North China Institute of Science and Technology, Beijing 101601, China

<sup>2</sup>School of Safety Science and Engineering, Henan Polytechnic University, Jiaozuo 454003, China

Correspondence should be addressed to Tao Yang; yangtao@ncist.edu.cn

Received 3 November 2020; Revised 27 January 2021; Accepted 1 February 2021; Published 17 February 2021

Academic Editor: Loupasakis Constantinos

Copyright © 2021 Wang Haidong et al. This is an open access article distributed under the Creative Commons Attribution License, which permits unrestricted use, distribution, and reproduction in any medium, provided the original work is properly cited.

Coal seam water injection is an important technical method to prevent and control coal and gas outburst and other disasters. Water can soften coal and change its mechanical properties. In order to study the mechanical properties of coal samples with different moisture content, briquette coal samples with five moistures content (4%, 6%, 8%, 10%, and 12%) were selected to carry out triaxial compression tests under different confining pressures (0.1, 0.2, 0.4, 0.8, and 1.2 MPa). Then, the mechanical response mechanism of the water-bearing briquette coal was analyzed. The results show that the slope of the linear elastic stage of the stress-strain curve gradually decreases with the increase of moisture content. Water-bearing coal exhibits strain strengthening characteristics under high confining pressure, which transforms the water-bearing coal from brittle to ductile state. The peak stress under different moisture content conditions shows a linear relationship with the confining pressure. The internal friction angle decreases linearly with the increase of moisture content. The cohesion varies parabolically with the increase of moisture content and reaches the maximum value when the moisture content is 8%. The coal body with moisture content between 7% and 9% has a high bonding force, which is beneficial to the consolidation of the coal body. Therefore, ensuring a reasonable moisture content of coal through coal seam injection can provide a basis for preventing coal and gas outburst.

## 1. Introduction

Coal and gas outburst and rock burst are relatively serious disasters in coal mines, which causes significant property losses and casualties [1–5]. Water injection is an important industrial measure to prevent these disasters and has been widely used in coal mines [6, 7]. The main factors affecting water injection effect are water injection pressure, water injection time, coal moisture content, and so on. There is a certain amount of original moisture in residual coal in goaf, which plays a softening role in the mechanical properties of coal. Therefore, it is of great significance to study the influence of different moisture content on the mechanical properties of coal.

Coal is a typical porous medium, which contains a multiscale pore structure [8]. When the pore pressure and consolidation pressure change, the moisture content [9, 10] and matrix adsorption expansion/contraction [11, 12] on the permeability of coal will also change, eventually

making the pore structure and mechanical properties of coal become more complex. Many scientists have carried out experiments on the mechanical properties of coal samples with different moisture content [13–19]. The reason why coal seam with high moisture content can effectively prevent coal and gas outburst is that coal has a stronger adsorption capacity for water molecules than methane molecules [20–22]. It is found that the moisture content is negatively related to the gas desorption rate and diffusion coefficient, resulting in less methane desorption amount [23]. Some scholars had pointed out that the intensity of coal and gas outburst decreases with the increase of original moisture content [24]. Through variable angle shear test, Yao et al. (2020) analyzed the variation law of shear strength, peak shear strain, cohesion and internal friction angle of coal samples with moisture content (0%, 7.10%, 15.68%, 22.90%, and 23.09%) and, on this basis, discussed the influence of moisture content on Mohr-Coulomb criterion [9]. Chen et al. (2019) studied

the triaxial compression and acoustic emission characteristics of gas-bearing coal under different water treatment conditions and analyzed how water affects the mechanical behavior of gas-bearing coal [25]. Talapatra et al. (2020) revealed the evolution law of coal deformation and strain and described the influence of moisture content on the permeability of coal through porous media in wet reservoir [26]. Chen et al. (2019) studied the influence of water-coal interaction on the mechanical strength of coal [27]. The results showed that with the increase of continuous wetting time and the number of dry and wet cycles, the peak stress and elastic modulus decreased and the peak strain increased. Zhang et al. (2018) carried out the compressive strength test of coal and analyzed how moisture affects the lignite strength [13]. Yang et al. (2019) studied the relationship between the moisture content of coal and the modulus of elasticity and the uniaxial compressive strength, and he found that there was a significant negative correlation between them [28]. All the above literatures studied the macroscopic mechanical property changes of coal samples from the experimental point of view. From a microscopic point of view, Gu et al. (2019) believe that the influence of moisture content on the mechanical properties of soft coal can be simplified as the influence on the interparticle bonding force [29]. He pointed out that the liquid bridging force between coal particles is composed of static bridging force and dynamic bridging force, and the effect of liquid bridging force can explain the influence of moisture content on soft coal with different porosity. Under dynamic loads, the dynamic bridging force cannot be ignored due to the fast relative motion between particles [30]. Ahamed et al. (2019) have made an in-depth study of how minerals and organic matter in coal interact with each other in the presence of water from the perspective of coal's chemical structure and elemental composition [31]. To sum up, the change of water environment leads to different moisture content in coal and also causes various changes in the microstructure and macroscopic mechanical properties of coal.

Coal is a typical heterogeneous rock whose mechanical properties are affected by many factors [32, 33]. Due to the special properties of coal, the research on the influence of water on its mechanical properties will always be a long-term and in-depth research subject. In the field of rock mechanics, it is generally believed that water will reduce the strength and elasticity of rock, but due to the special properties of coal, the effect of water on its mechanical properties needs to be further studied. Most of the existing researches on the mechanical properties of coal samples were focused on uniaxial compression, without considering the confining pressure and multiaxial compression. In addition, due to the difficulty in preparing water-bearing coal samples, coal samples with low moisture content are mostly selected in some literatures to study [6, 26, 29, 34]. At present, the scale of moisture content of experimental coal samples is not wide enough. It is necessary to consider a broader scale of moisture content to further study the effects of moisture content on elastic parameters, plastic deformation, and peak strength of experimental coal samples.

In response to the above, five kinds of briquette coal samples with different moisture content were prepared and triaxial compression experiments were conducted to observe the effect of moisture on the mechanical properties of coal. The effects of moisture content and confining pressure on stress-strain, peak stress, elastic modulus, Poisson's ratio, cohesion, and internal friction angle were analyzed. This paper aims to analyze and evaluate the mechanical behavior of coal under different moisture content.

## 2. Experimental

**2.1. Coal Sample Selection.** The experimental coal samples were taken from Baiping Coal Mine in Dengfeng City, Henan Province, China. The minefield is about 10 km long from east to west, 2-4 km wide from south to north, covering an area of about 18.37 km<sup>2</sup>. The average coal thickness is 5.3 m. Coal seam exists in the form of powder and scale, mainly in the form of pulverized coal with low strength (the hardness coefficient of proctor is about 0.5-0.8 before water injection). The coal seam is in the form of powder by hand twisting, which belongs to the poor coal with medium calorific value and extra high calorific value. The industrial analysis results of the coal sample are shown in Table 1.

**2.2. Preparation of Briquette with Different Moisture Content.** The main purpose of this paper is to study the mechanical properties of briquette coal samples with different moisture content. Although the mechanical properties of briquette and raw coal are not exactly the same, there are great similarities in the mechanical laws of briquette coal [35]. Briquette is favored by many scholars because of its good repeatability [36-39]. This paper also conducts a series of experiments on briquette coal. By adding different water mass into the coal sample, rock pressure experimental system is used to press the formed coal under the condition of axial pressure, as shown in Figure 1. The specific preparation steps are as follows:

- (1) Turn on the computer power supply, start the oil pressure power switch, run the YAD-2000 micro-computer controlled electro-hydraulic servo rock pressure experiment system, place the bottom hydraulic cylinder of the laboratory at the lowest displacement, and the upper vertical pressure cylinder at the appropriate position, so as to place the forming mold in the tester
- (2) Select lean coal sample within  $0.2 \text{ mm} < d < 1 \text{ mm}$  and  $1 \text{ mm} < d < 3 \text{ mm}$ , dry for 24 h, then use electronic balance to weigh 300 g under peeling condition, and put it into plastic mixer; use beaker to weigh a certain amount of water, spray water into plastic mixer with sprayer, and spray while stirring, so as to fully mix coal particles and water. The calculation formula of moisture content is [40]:

$$w = \frac{m_2 - m_1}{m_2} \times 100\%, \quad (1)$$

TABLE 1: Industrial analysis results of raw coal.

Coal mine	Coal rank	$M_{ad}/\%$	$A_{ad}/\%$	$V_{ad}/\%$	Hydraulic conductivity/( $m^2 \cdot d^{-1}$ )	Contact angle/ $^\circ$
Baiping	Lean coal	0.96	10.28	15.06	0.905	33.2

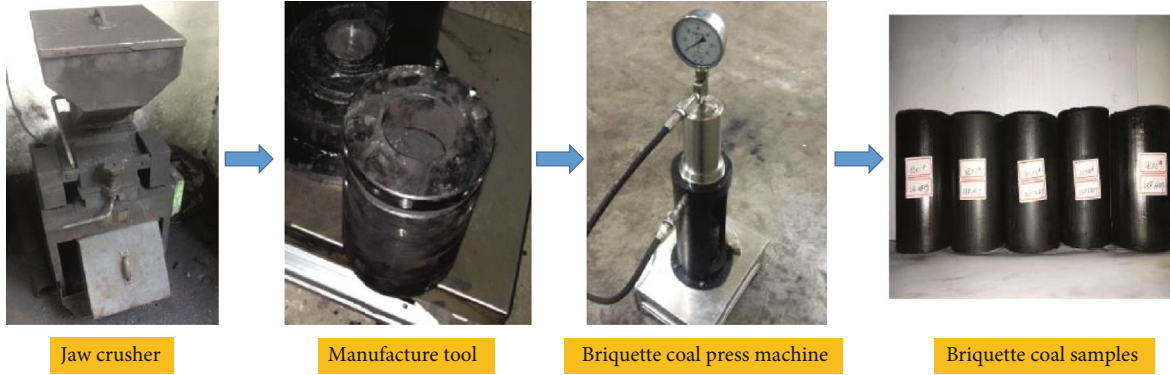


FIGURE 1: Preparation steps of briquette coal sample.

where  $m_1$  refers to the dried mass of coal sample, g;  $m_2$  refers to the coal sample mass added with purified water, g;  $w$  stands for the moisture content, %.

- (3) The base of the mold is placed on the test bench. In order to ensure the flatness of the lower surface of the formed coal sample, a thin paper with a diameter of about 49 mm is placed on the base, and a stainless steel cylinder with an inner diameter of 50 mm is placed. The mold is formed by mixing the prepared coal sample with coal and water with an iron spoon, and then, the coal sample mold is formed by using a thin rod cylinder, and the diameter of the upper end of the mold is about 49.95 mm. The bottom bearing cylinder plane is located in the cylinder. Then, place the whole die on the testing machine
- (4) Operate the testing machine software according to the steps, set it as the displacement control mode, and finally set the setting displacement speed of 0.05 mm/s after many experiments; set the protection pressure of 100 MPa, and control the molding pressure of the testing machine within 30 min
- (5) In order to ensure the formability, the prepared briquette coal has a high molding rate, and the demolding speed is set as displacement control with a speed of 5 mm/s. A layer of crumpled and curled plastic film is placed in the demolding cylinder. On the one hand, a certain supporting force is given to the separated briquette to ensure that the supporting force in the demolding process and the compressive strength of the briquette itself are greater than its own gravity; on the other hand, when the briquette coal is completely detached, it can prevent the bottom from falling off and damage, resulting in uneven end face

- (6) The prepared coal samples with different moisture content (see Figure 1) were coated with 4-5 layers of fresh-keeping film to prevent water loss

**2.3. Triaxial Compression Experiment System and Scheme.** The experiment work uses the MTS815.2 test system, as shown in Figure 2. The experimental system is mainly composed of the main machine, multichannel controller, confining pressure control cabinet, pore pressure control cabinet, hydraulic oil source, main control computer, etc. The maximum load of the system equipment is 1700 kN, and the maximum confining pressure is 45 MPa. The whole process is controlled by computer, which can automatically collect and process relevant data. It can be used to test the stress-strain curve of single axis and triaxial and the effect of pore water pressure on rock deformation and strength.

Firstly, the pulverizer was used to crush the coal samples, and the coal particles with the particle size of  $0.2 \text{ mm} < d < 1 \text{ mm}$  and  $1 \text{ mm} < d < 3 \text{ mm}$  were taken. The coal samples with two particle sizes were mixed according to the mass ratio of 1:1 and put into the dryer for 12 h. The method of spraying small aperture pure water and fully mixing was used to humidify the coal sample. After sufficient wetting for a certain period of time, the standard coal sample of  $\Phi 50 \text{ mm} \times 100 \text{ mm}$  was pressed into the forming mold under the action of the testing machine and the pressure of 100 MPa. The allowable variation range of specimen height is 95-105 mm. In the experiment, we found that it is difficult to form coal with moisture content lower than 4% or higher than 12%. Therefore, the briquette coals with moisture content of 4%, 6%, 8%, 10%, and 12% were used to study the mechanical properties of briquette coals. In order to test the deformation and strength characteristics of different moisture content under different confining pressures (0, 0.1, 0.2, 0.4, 0.8, and 1.2 MPa), 90 processed and formed cylinder standard coal samples were taken, and each moisture content was



FIGURE 2: MTS815.2 test system.

repeated with three test pieces under one confining pressure for triaxial loading test, with unified number and sequential number. In order to ensure that the displacement and strain of the specimen increase only after the peak strength, the axial displacement control mode is adopted in the whole loading process to obtain the whole stress-strain curve of the specimen. The loading speed is 0.005 mm/s, and the experimental data is automatically recorded by the testing machine.

### 3. Results and Analysis

The relationship between axial stress-strain curve and confining pressure under different moisture content conditions is shown in Figure 3. As can be seen, in the case of fixed confining pressure, with the increase of moisture content, the slope of linear elastic stage decreases as a whole, and the bearing deformation limit increases. This indicates that the elastic modulus decreases and the plasticity increases. With the increase of moisture content, the plasticity increases, the elastic potential is consumed, and the plastic deformation of coal sample occurs. It can reduce the accumulation of energy in the coal body and avoid the sudden release of energy, which is conducive to the prevention and control of coal and gas outburst [41]. When the moisture content is 4%, 6%, and 8%, respectively, the low confining pressure (0, 0.1, 0.2, and 0.4 MPa) exhibits strain-softening characteristics, and the high confining pressure (0.8 and 1.2 MPa) shows strain strengthening characteristics. With the increase of confining pressure, water-bearing coal changes from brittleness to ductility. At 10% and 12% of moisture content, the postpeak curve of water-bearing coal changes from plastic flow state to strain strengthening stage with the increase of confining pressure. When the moisture content is between 4% and 8%, the coal with moisture content is plastic-elastic-plastic body when the confining pressure is between 0 MPa and 1.2 MPa. The briquette coal with moisture content between 10% and 12% can be regarded as a typical elastic-plastic body.

It shows that under the condition of reasonable confining pressure and moisture content, it is beneficial to the transformation of water-bearing coal from brittleness to ductility and to the release of energy. Literature [42] also supports our views to some extent. In the process of coal mining, the horizontal stress from three-way hydrostatic state will gradually be low to 0 from coal seam depth to the working face. Stress redistribution in front of the coal body is a time-dependent process. The method to control the confining pressure is to maintain the reasonable mining speed, so as to prevent coal and gas outburst and rock burst disaster.

Figure 4 shows the peak value change of axial stress with the moisture content under different confining pressures. It can be seen that the yield stress and peak strength of water-bearing coal increase gradually with the increase of confining pressure. With the increase of moisture content, the axial support stress of water-bearing coal increases first and then decreases, and the larger the confining pressure is, the more obvious the trend is. This may be due to the formation of thick water film on the surface of coal particles in the process of briquetting, which makes the contact between particles not close and reduces the compressive strength of briquette coal. When the confining pressure is 0, 0.1, and 0.4 MPa, the axial stress reaches the peak value when the moisture content is 8%. When the confining pressure is 0.2, 0.8, and 1.2 MPa, the axial stress reaches the peak value when the moisture content is 6%.

Here, the peak stress and confining pressure data of briquette under different moisture content were fitted in Figure 5. As indicated in Figure 5, when the moisture content is 4%, 6%, 10%, and 12%, the linear goodness of fit of stress peak value and confining pressure is greater than 0.98, showing a significant linear relationship between them. Similar conclusions have been reached in some literature [37, 43]. When the moisture content is 8%, the goodness of fit is greater than 0.96. Based on the generalized Hoek Brown criterion and tangent method theory, the cohesion  $c$  and internal friction angle  $\Phi$  of rock can be approximately determined. According to the

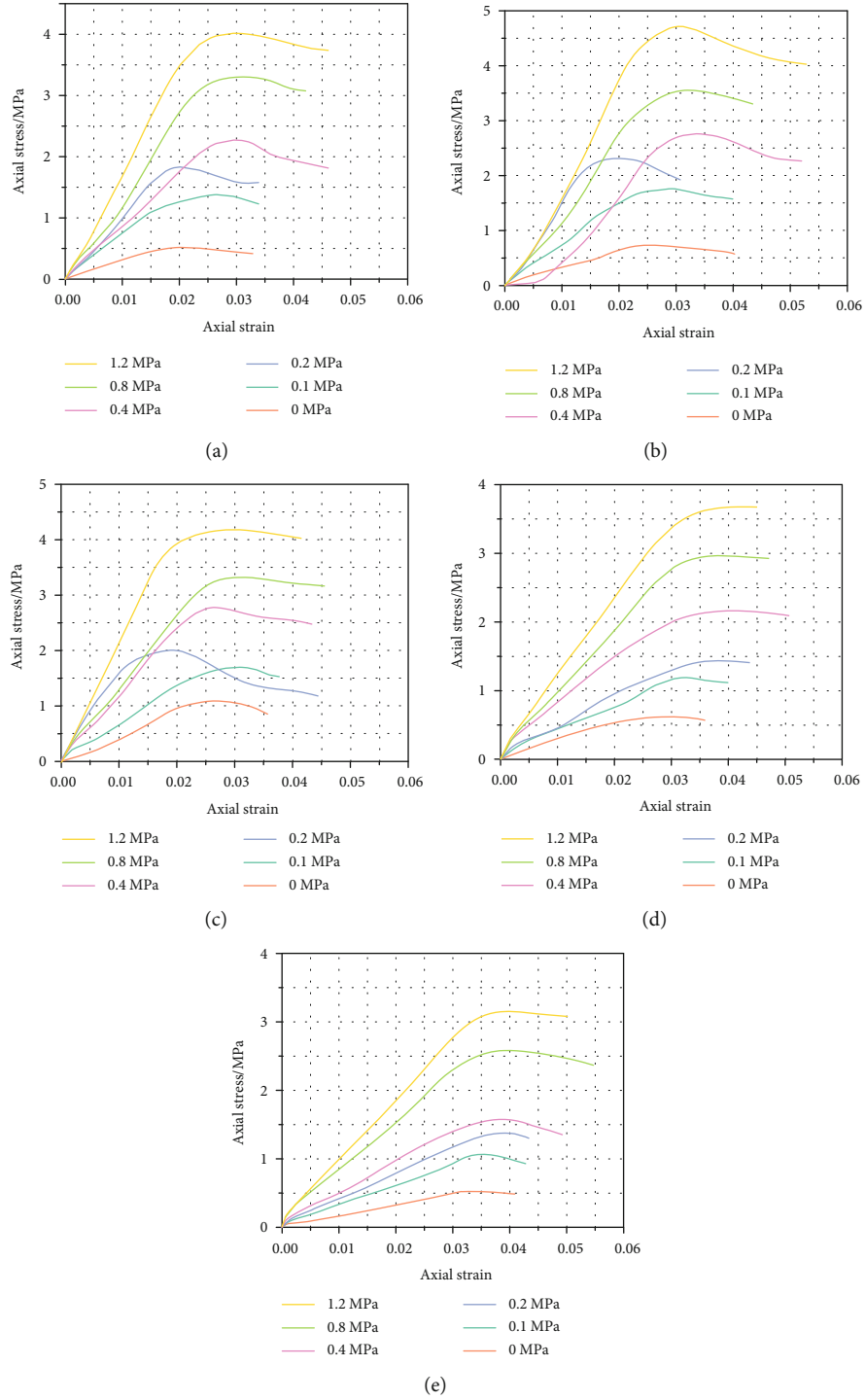


FIGURE 3: Relationship between axial stress-strain curve and confining pressure under different moisture content conditions. (a) Moisture content 4%. (b) Moisture content 6%. (c) Moisture content 8%. (d) Moisture content 10%. (e) Moisture content 12%.

peak strength of Coulomb criterion  $\sigma_s = a + b\sigma_3$  ( $\sigma_s$  is the peak stress and  $\sigma_3$  is the confining pressure), and the values of  $a$  and  $b$  in the fitting equation in Figure 5,  $\Phi$  and  $c$  can be calculated based on Eq. (2) and (3).

$$\phi = \arcsin \frac{b-1}{b+1}, \quad (2)$$

$$c = \frac{a(1 - \sin \phi)}{2 \cos \phi}. \quad (3)$$

The change trend of elastic modulus and Poisson's ratio of briquette with moisture content is tested, as shown in Figure 6. It can be seen from Figure 6(a) that the elastic modulus of briquette first increases and then decreases with the increase of moisture content, and the fitting equation is  $\gamma = -0.138 +$

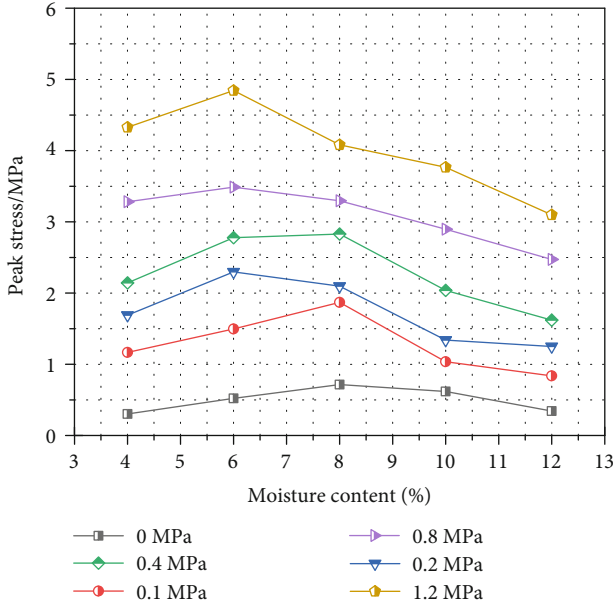


FIGURE 4: Relationship between peak stress and moisture content under different confining pressures.

$0.329x - 0.021x^2$ . When the moisture content is about 8%, the modulus of elasticity of briquette reaches the maximum, which is 1.17 GPa. When the moisture content is between 4% and 8%, with the increase of moisture content, the elastic modulus of briquette increases, the bearing capacity and the rigid mechanical properties of briquette increase. When the moisture content is more than 8%, the elastic modulus of briquette decreases, the bearing capacity decreases, and the plasticity of briquette increases with the increase of moisture content. Poisson's ratio is the ratio of transverse strain to longitudinal strain, which is the elastic constant reflecting transverse deformation. It can be seen from Figure 6(b) that the elastic modulus of briquette increases first and then decreases with the increase of moisture content, and the fitting equation is  $y = 0.599 - 0.087x + 0.005x^2$ . When the moisture content of briquette is 8%, the Poisson's ratio of briquette is at the minimum, which is 0.218. When the moisture content is between 4% and 8%, the Poisson's ratio of briquette decreases with the increase of moisture content. When the moisture content is more than 8%, the Poisson's ratio increases gradually with the increase of moisture content, and the transverse strain trend of briquette increases.

Furthermore, we investigated the change trend of cohesion and internal friction angle with moisture content, as shown in Figure 7. From Figure 7, we can conclude that the internal friction angle decreases linearly with the increase of moisture content. Yao et al. (2020) believed that the internal friction angle and the moisture content show a negative exponential decrease trend [9], which is mainly due to the difference of the fitting equation. But in essence, the relationship between the internal friction angle studied in this paper and the change of water is consistent with their research results. With the increase of moisture content, the cohesive force shows a parabola

shape with a secondary opening downward, which increases first and then decreases. The cohesion reaches the maximum value when the moisture content is 8%. The moisture content is from 4% to 8%, the internal friction angle is reduced from  $28.385^\circ$  to  $24.186^\circ$ , and the reduction rate is 14.793%. Under the same conditions, the cohesion is increased from 0.297 MPa to 0.514 MPa, and the increase rate is 73.06%, i.e., the influence of moisture content on cohesion is greater than that on internal friction angle. Compared with coal molecules, the cohesion and liquid bridge force between water molecules play an important role. Under the action of dynamic load, due to the fast relative motion between particles, the hydrodynamic bridging force cannot be ignored [29, 30]. The water cohesion of the formed coal with the moisture content of 8% increases sharply, which may be caused by the macroscopic manifestation of the liquid bridge force between the wet particles. It had been reported out that when the external moisture content of raw coal is between 7% and 14%, the water mainly exists in the swing state between the particle pores, and the distribution of discontinuous liquid bridge between the swing state particles, including dynamic liquid bridge force and static liquid bridge force [44]. Therefore, we focused on the peak strength with a moisture content of 8%.

The stress-strain curves of the coal sample with 8% moisture after loading were extracted, as illustrated in Figure 8. Among them, the axial stress is  $\sigma_1$ , the confining pressure is  $\sigma_3$ , the axial strain is  $\varepsilon_1$ , the radial strain is  $\varepsilon_3$ , and the volume strain is  $\varepsilon_v$ . Axial strain is positive in compression, while radial strain and volume strain are positive in expansion. The specific analysis is as follows:

- (1)  $\sigma_1 - \varepsilon_1$  Curve. The whole process is characterized by compaction, elastic and plastic failure. Before the peak stress, the stress-strain curve changes from linear elasticity to linear elasticity with the increase of confining pressure, indicating that the axial deformation characteristics of the specimen are related to  $\sigma_1 - \sigma_3$ . With the increase of the difference value of  $\sigma_1 - \sigma_3$ , the slope of the curve increases significantly, the failure load increases, and the plastic deformation increases obviously. The results show that coal strength containing moisture content increases with the increase of confining pressure, which shows as the compressive type. The slope of the curve before the peak of the confining pressure of 0.1 MPa increases first, then decreases, and then increases. The possible reason is that there is a large crack between the large coal particle and the small coal particle in the process of forming under the constant load. Under the stress, the crack is further closed. The curve shows the same stress rate and produces a large displacement. After the peak stress, with the increase of confining pressure, the postpeak curve changes from strain softening to strain strengthening. Meanwhile, the residual strength also increases, and the peak stress corresponding to the peak strain value increases accordingly. This shows that the coal

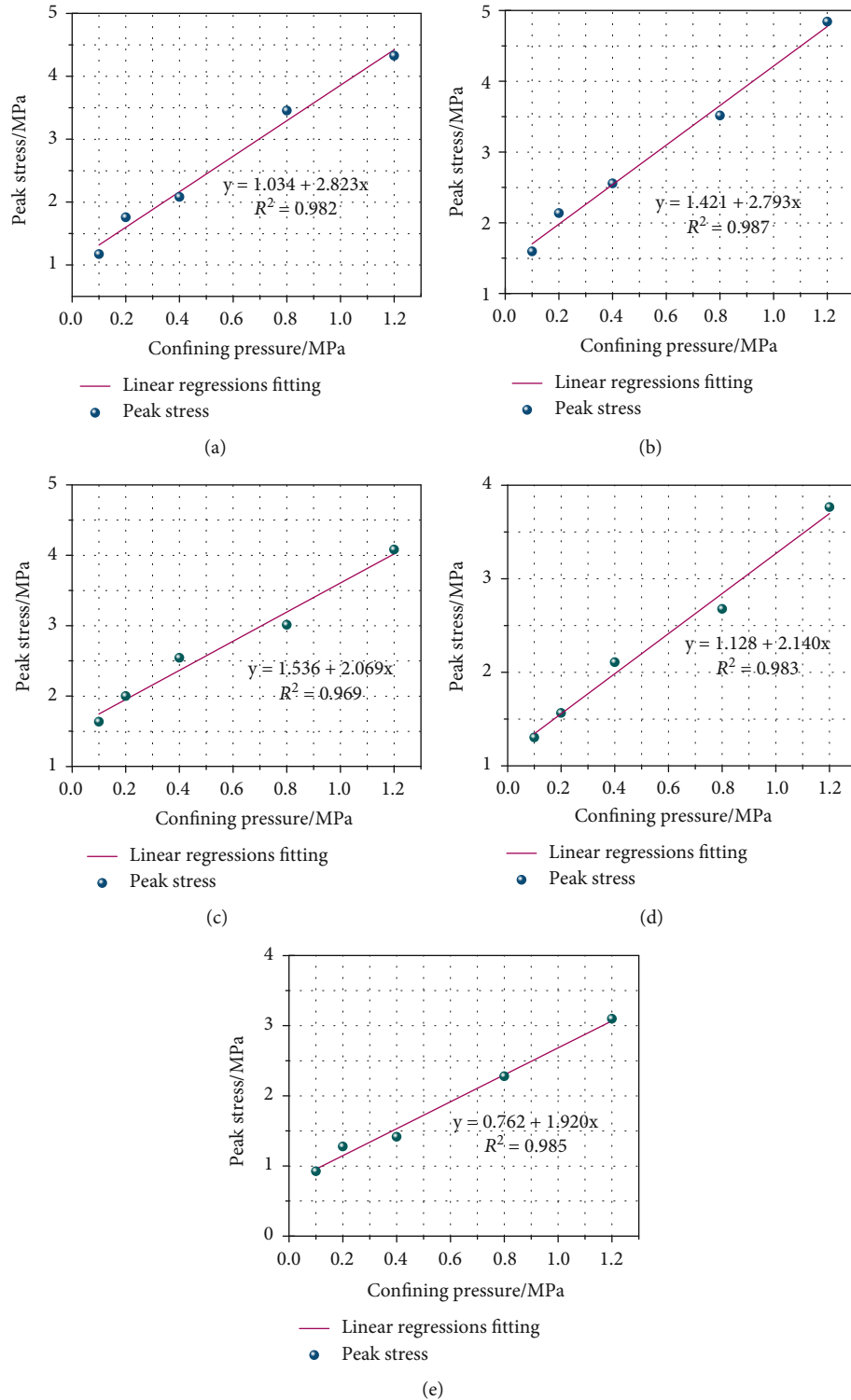


FIGURE 5: Relationship between stress peak value and confining pressure under different moisture content conditions. (a) Moisture content 4%. (b) Moisture content 6%. (c) Moisture content 8%. (d) Moisture content 10%. (e) Moisture content 12%.

body after water injection faces to the deep part of the coal body from the mining work. Under the effect of in situ stress, the coal wall shows the phenomenon of spalling and slag falling. While, the deep coal body changes to the plastic strengthening, showing the fracture and pore closure

(2)  $\sigma_1 - \varepsilon_3$  Curve. In the experiment, the stress intensity increases gradually with the increase of confining pressure under the same displacement condition. Under the same stress condition, with the increase of confining pressure, the radial displacement decreases correspondingly, and the corresponding

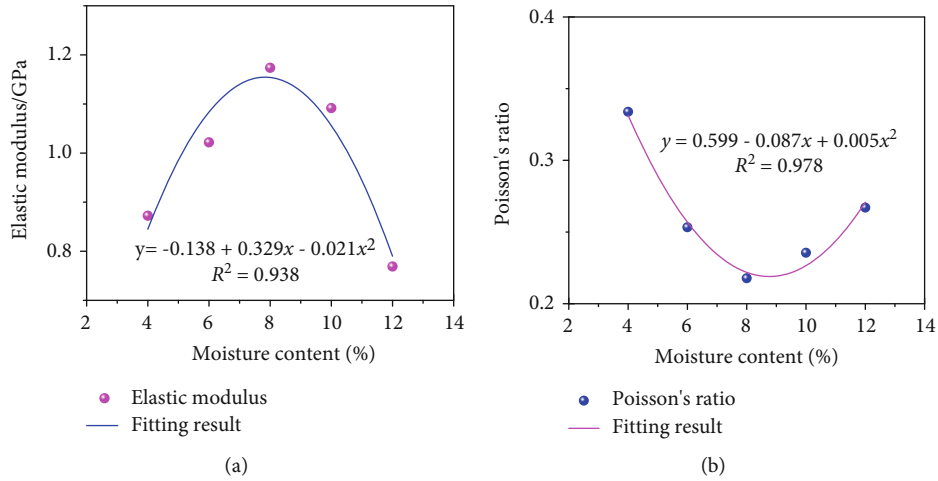


FIGURE 6: Relationship between moisture content and Elastic modulus and Poisson's ratio. (a) Change of Elastic modulus with moisture content. (b) Change of Poisson's ratio with moisture content.

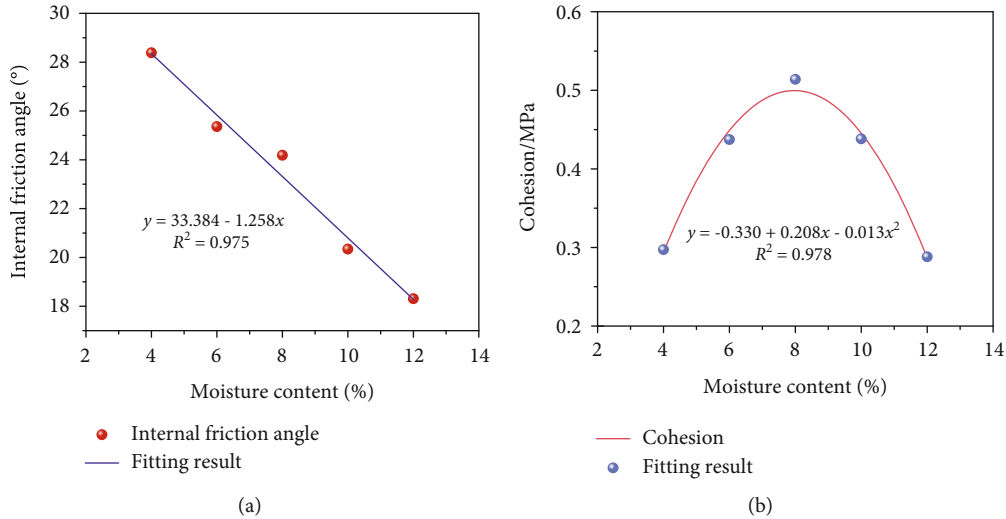


FIGURE 7: Relationship between moisture content and internal friction angle and cohesion. (a) Change of internal friction angle with moisture content. (b) Change of cohesion with moisture content.

strain rate of stress increases gradually, especially the confining pressure of 0.4 MPa to 1.2 MPa. This indicates that the horizontal displacement of the same ground stress of the injected coal seam is larger under low confining pressure, and the horizontal displacement is gradually reduced from the deep coal body to the surface of the coal wall. Under the action of the horizontal force, the horizontal displacement is expressed as the sheet side or the coal wall extrusion

- (3)  $\sigma_1 - \varepsilon_v$  Curve. The overall performance volume decreased first and then increased. With the increase of confining pressure, the volume strain  $\varepsilon_v$  of pore fracture structure increases first and then decreases. Although the volume of the specimen is decreasing, the volume changes rapidly, so the volume strain of

the specimen increases. When the slope of a certain point of the curve of  $\sigma_1 - \varepsilon_v$  is infinite, that is, when the volume of the test piece reaches the minimum value, it is called the elastic limit point. The crack growth of the specimen is stable, which conforms to Hooke's law and shows a linear elastic stage. When the axial stress reaches a certain value, that is, the volume of the specimen is equal to that of the original specimen, and then the axial stress increases, and  $\varepsilon_v$  increases until the compaction of the specimen is compacted. In this process, the volume change gradually decreases, and after entering the yield stage, the volume of briquette coal specimen increases, showing the phenomenon of expansion.  $\varepsilon_v$  of the specimen develops rapidly to the negative direction of displacement, and the displacement value in the negative



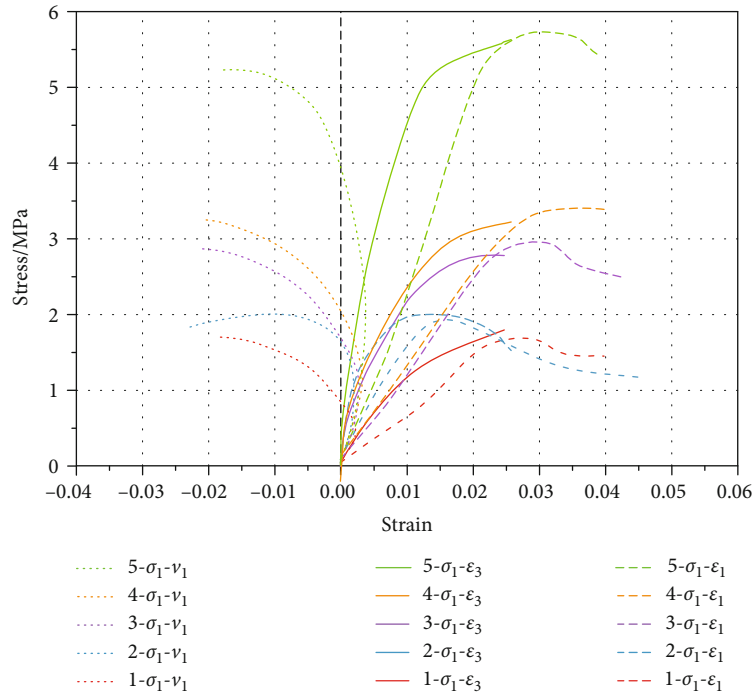


FIGURE 8: Stress-strain curve of water-bearing coal (8%) under different confining pressures.

direction is larger than that in the positive direction, and the volume of the specimen after failure is larger than that of the original specimen

#### 4. Conclusions

In this paper, the briquette coal samples with different moisture content are prepared, and the triaxial compression tests are carried out on the briquette coal samples under different confining pressures with MTS815.2 testing machine. The mechanical properties of the coal samples with different moisture content are studied. The main conclusions are as follows:

- (1) When the moisture content is fixed, the confining pressure can strengthen the mechanical properties of the coal. When the moisture content is less than 8%, there is a small downward concave curve, and when the moisture content is greater than 8%, the curve shows good linear elasticity. Moisture content is 4%, 6%, and 8%. Low confining pressure (0, 0.1, 0.2, and 0.4 MPa) shows strain-softening characteristics; high confining pressure (0.8 and 1.2 MPa) shows strain strengthening characteristics
- (2) Under the same confining pressure, with the increase of moisture content, the peak strength of briquette coal increases first and then decreases. The peak stress and confining pressure show a linear positive correlation. With the increase of moisture content, the internal friction angle of briquette coal decreases linearly; the cohesion first increases and then decreases with the increase of moisture content

- (3) The influence of moisture content in the coal sample on cohesion is greater than that of the internal friction angle. When the moisture content is 8%, the cohesion of the coal sample is the largest, the consolidation ability of the coal body is strong, and the risk of coal and gas outburst is correspondingly reduced

By studying the physical and mechanical properties of coal bodies with different moisture content, we hope to provide some theoretical and field engineering guidance for improving the understanding of the mechanism of gas outburst prevention by coal seam water injection, standardizing coal seam water injection technology, and coal mine gas prevention.

#### Data Availability

The data used to support the findings of this study are available from the corresponding author upon request.

#### Conflicts of Interest

The authors declare that they have no conflicts of interest.

#### Acknowledgments

The research was supported by the National Natural Science Foundation of China (Project No. 51974127).

#### References

- [1] W. Yang, H. Wang, B. Lin et al., "Outburst mechanism of tunnelling through coal seams and the safety strategy by using

- “strong-weak” coupling circle-layers,” *Tunnelling and Underground Space Technology*, vol. 74, pp. 107–118, 2018.
- [2] H. Wang, Y. Cheng, and L. Yuan, “Gas outburst disasters and the mining technology of key protective seam in coal seam group in the Huainan coalfield,” *Natural Hazards*, vol. 67, no. 2, pp. 763–782, 2013.
  - [3] Y. Fujii, Y. Ishijima, Y. Ichihara et al., “Mechanical properties of abandoned and closed roadways in the Kushiro Coal Mine, Japan,” *International Journal of Rock Mechanics and Mining Sciences*, vol. 48, no. 4, pp. 585–596, 2011.
  - [4] M. B. Díaz Aguado and C. González Nicieza, “Control and prevention of gas outbursts in coal mines, Riosa-Olloniego coalfield, Spain,” *International Journal of Coal Geology*, vol. 69, no. 4, pp. 253–266, 2007.
  - [5] J. Lin, Y. Zuo, K. Zhang et al., “Coal and gas outburst affected by law of small fault instability during working face advance,” *Geofluids*, vol. 2020, 12 pages, 2020.
  - [6] C. Wang, S. Yang, J. Li, X. Li, and C. Jiang, “Influence of coal moisture on initial gas desorption and gas-release energy characteristics,” *Fuel*, vol. 232, pp. 351–361, 2018.
  - [7] Z. Xiao and Z. Wang, “Experimental study on inhibitory effect of gas desorption by injecting water into coal-sample,” *Procedia Engineering*, vol. 26, pp. 1287–1295, 2011.
  - [8] Y. Li, J. Yang, Z. Pan, and W. Tong, “Nanoscale pore structure and mechanical property analysis of coal: an insight combining AFM and SEM images,” *Fuel*, vol. 260, p. 116352, 2020.
  - [9] Q. Yao, C. Tang, Z. Xia et al., “Mechanisms of failure in coal samples from underground water reservoir,” *Engineering Geology*, vol. 267, p. 105494, 2020.
  - [10] J. Wang, Z. Wan, Y. Wang et al., “Effect of stress and moisture content on permeability of gas-saturated raw coal,” *Geofluids*, vol. 2020, 13 pages, 2020.
  - [11] Y. Li, Z. Wang, Z. Pan, X. Niu, Y. Yu, and S. Meng, “Pore structure and its fractal dimensions of transitional shale: a cross-section from east margin of the Ordos Basin, China,” *Fuel*, vol. 241, pp. 417–431, 2019.
  - [12] Y. Li, Y. Wang, J. Wang, and Z. Pan, “Variation in permeability during CO<sub>2</sub>-CH<sub>4</sub> displacement in coal seams: part 1 – experimental insights,” *Fuel*, vol. 263, p. 116666, 2020.
  - [13] X. Zhang, R. P. Gamage, M. S. A. Perera, and A. S. Ranathunga, “Effects of water and brine saturation on mechanical property alterations of brown coal,” *Energies*, vol. 11, no. 5, p. 1116, 2018.
  - [14] X. Chen and G. Yao, “An improved model for permeability estimation in low permeable porous media based on fractal geometry and modified Hagen-Poiseuille flow,” *Fuel*, vol. 210, pp. 748–757, 2017.
  - [15] V. Vishal, P. G. Ranjith, and T. N. Singh, “An experimental investigation on behaviour of coal under fluid saturation, using acoustic emission,” *Journal of Natural Gas Science and Engineering*, vol. 22, pp. 428–436, 2015.
  - [16] B. A. Poulsen, B. Shen, D. J. Williams, C. Huddleston-Holmes, N. Erarslan, and J. Qin, “Strength reduction on saturation of coal and coal measures rocks with implications for coal pillar strength,” *International Journal of Rock Mechanics and Mining Sciences*, vol. 71, pp. 41–52, 2014.
  - [17] H. Qin, G. Huang, and W. Wang, “Experimental study of acoustic emission characteristics of coal samples with different moisture contents in process of compression deformation and failure,” *Chinese Journal of Rock Mechanics and Engineering*, vol. 31, no. 6, pp. 1115–1120, 2012.
  - [18] M. S. A. Perera, P. G. Ranjith, and M. Peter, “Effects of saturation medium and pressure on strength parameters of Latrobe Valley brown coal: Carbon dioxide, water and nitrogen saturations,” *Energy*, vol. 36, no. 12, pp. 6941–6947, 2011.
  - [19] X. Zhang, P. G. Ranjith, Y. Lu, and A. S. Ranathunga, “Experimental investigation of the influence of CO<sub>2</sub> and water adsorption on mechanics of coal under confining pressure,” *International Journal of Coal Geology*, vol. 209, pp. 117–129, 2019.
  - [20] Z. Shi-yin and S. Shu-xun, “Physical chemistry mechanism of influence of liquid water on coalbed methane adsorption,” *Procedia Earth and Planetary Science*, vol. 1, no. 1, pp. 263–268, 2009.
  - [21] B. B. Beamish and P. J. Crosdale, “Instantaneous outbursts in underground coal mines: an overview and association with coal type,” *International Journal of Coal Geology*, vol. 35, no. 1–4, pp. 27–55, 1998.
  - [22] C. Laxminarayana and P. J. Crosdale, “Role of coal type and rank on methane sorption characteristics of Bowen Basin, Australia coals,” *International Journal of Coal Geology*, vol. 40, no. 4, pp. 309–325, 1999.
  - [23] X. Chen and Y. Cheng, “Influence of the injected water on gas outburst disasters in coal mine,” *Natural Hazards*, vol. 76, no. 2, pp. 1093–1109, 2015.
  - [24] J. Geng, J. Xu, W. Nie, S. Peng, C. Zhang, and X. Luo, “Regression analysis of major parameters affecting the intensity of coal and gas outbursts in laboratory,” *International Journal of Mining Science and Technology*, vol. 27, no. 2, pp. 327–332, 2017.
  - [25] M. Y. Chen, Y. P. Cheng, J. C. Wang, H. R. Li, and N. Wang, “Experimental investigation on the mechanical characteristics of gas-bearing coal considering the impact of moisture,” *Arabian Journal of Geosciences*, vol. 12, no. 18, pp. 1–15, 2019.
  - [26] A. Talapatra and M. M. Karim, “The influence of moisture content on coal deformation and coal permeability during coalbed methane (CBM) production in wet reservoirs,” *Journal of Petroleum Exploration and Production Technology*, vol. 10, no. 5, pp. 1907–1920, 2020.
  - [27] S. Chen, T. Jiang, H. Wang, F. Feng, D. Yin, and X. Li, “Influence of cyclic wetting-drying on the mechanical strength characteristics of coal samples: a laboratory-scale study,” *Energy Science & Engineering*, vol. 7, no. 6, pp. 3020–3037, 2019.
  - [28] W. Yang, H. Wang, Q. Zhuo et al., “Mechanism of water inhibiting gas outburst and the field experiment of coal seam infusion promoted by blasting,” *Fuel*, vol. 251, pp. 383–393, 2019.
  - [29] H. Gu, M. Tao, W. Cao, J. Zhou, and X. Li, “Dynamic fracture behaviour and evolution mechanism of soft coal with different porosities and water contents,” *Theoretical and Applied Fracture Mechanics*, vol. 103, p. 102265, 2019.
  - [30] D. Y. C. Chan and R. G. Horn, “The drainage of thin liquid films between solid surfaces,” *The Journal of Chemical Physics*, vol. 83, no. 10, pp. 5311–5324, 1985.
  - [31] M. A. A. Ahamed, M. S. A. Perera, S. K. Matthai, P. G. Ranjith, and L. Dong-yin, “Coal composition and structural variation with rank and its influence on the coal-moisture interactions under coal seam temperature conditions – a review article,” *Journal of Petroleum Science and Engineering*, vol. 180, pp. 901–917, 2019.
  - [32] A. Marzec, “Towards an understanding of the coal structure: a review,” *Fuel Processing Technology*, vol. 77–78, pp. 25–32, 2002.

- [33] H. Xu, G. Wang, C. Fan, X. Liu, and M. Wu, "Grain-scale reconstruction and simulation of coal mechanical deformation and failure behaviors using combined SEM Digital Rock data and DEM simulator," *Powder Technology*, vol. 360, no. 1, pp. 1305–1320, 2020.
- [34] H. Gu, M. Tao, X. Li, A. Momeni, and W. Cao, "The effects of water content and external incident energy on coal dynamic behaviour," *International Journal of Rock Mechanics and Mining Sciences*, vol. 123, p. 104088, 2019.
- [35] X. Wang, W. Xie, Z. Su, and Q. Tang, "Experimental development of coal-like material with solid-gas coupling for quantitative simulation tests of coal and gas outburst occurred in soft coal seams," *Processes*, vol. 7, no. 3, p. 155, 2019.
- [36] H. Wang and J. Li, "Mechanical behavior evolution and damage characterization of coal under different cyclic engineering loading," *Geofluids*, vol. 2020, 19 pages, 2020.
- [37] J. Lu, G. Yin, D. Zhang, H. Gao, C. Li, and M. Li, "True triaxial strength and failure characteristics of cubic coal and sandstone under different loading paths," *International Journal of Rock Mechanics and Mining Sciences*, vol. 135, p. 104439, 2020.
- [38] H. Zhao, T. Wang, H. Zhang, and Z. Wei, "Comparison of local load influence on crack evolution of coal and briquette coal samples," *Advances in Civil Engineering*, vol. 2018, 12 pages, 2018.
- [39] Y. Geng, D. Tang, H. Xu et al., "Experimental study on permeability stress sensitivity of reconstituted granular coal with different lithotypes," *Fuel*, vol. 202, pp. 12–22, 2017.
- [40] Q. Yao, W. Wang, L. Zhu, Z. Xia, C. Tang, and X. Wang, "Effects of moisture conditions on mechanical properties and AE and IR characteristics in coal-rock combinations," *Arabian Journal of Geosciences*, vol. 13, no. 14, 2020.
- [41] S. Zhou and B. Lin, *The Theory of Gas Flow and Storage in Coal Seams*, Coal Industry Publishing House, Beijing, 1999.
- [42] Y. Liu, S. Li, D. Tang et al., "Mechanical behavior of low-rank bituminous coal under compression: an experimental and numerical study," *Journal of Natural Gas Science and Engineering*, vol. 66, pp. 77–85, 2019.
- [43] H. Xu, Y. Qin, G. Wang, C. Fan, M. Wu, and R. Wang, "Discrete element study on mesomechanical behavior of crack propagation in coal samples with two prefabricated fissures under biaxial compression," *Powder Technology*, vol. 375, no. 9, pp. 42–59, 2020.
- [44] K. Hotta, K. Takeda, and K. Iinoya, "The capillary binding force of a liquid bridge," *Powder Technology*, vol. 10, no. 4-5, pp. 231–242, 1974.